

## Impact response by a foamlike forest of coiled carbon nanotubes

Chiara Daraio, Vitali F. Nesterenko,<sup>a)</sup> and Sungho Jin

*Materials Science and Engineering Program, Mechanical and Aerospace Engineering Department, University of California, San Diego, La Jolla, California 92093-0411*

Wei Wang<sup>b)</sup> and Apparao M. Rao

*Department of Physics and Astronomy, Clemson University, Clemson, South Carolina 29634*

(Received 21 April 2006; accepted 5 July 2006; published online 22 September 2006)

We studied the dynamic response of a foamlike forest of coiled carbon nanotubes under high strain rate deformation using a simple drop-ball test. The method is based on measuring the dynamic force between the ball and the foam on the substrate during the stages of penetration and restitution. The analysis of the forest's morphology after impact has shown no trace of plastic deformation and a full recovery of the foamlike layer of coiled carbon nanotubes under various impact velocities. The contact force exhibits a strongly nonlinear dependence on displacement and appears fundamentally different from the response of a forest of straight carbon nanotubes, and from the Hertzian type of plane-sphere interaction. "Brittle" fracture of the foamlike layer is observed after repeated high velocity impacts. Such layers of coiled nanotubes may be used as a strongly nonlinear spring in discrete systems for monitoring their dynamic behavior and as a nanostructure for localized microimpact protection. © 2006 American Institute of Physics. [DOI: 10.1063/1.2345609]

### I. INTRODUCTION

The study of thin structural foams<sup>1</sup> for cushioning, energy dissipation, and protection has recently been receiving increasing attention for several practical applications, including mitigation of explosive loading.<sup>2</sup> Investigations on the dynamic response of foamlike forests of carbon nanotubes<sup>3,4</sup> have shown a strongly nonlinear response that appears very suitable for energy-absorbing layered material in noise and shock wave mitigation and as nonlinear springs for assembling nonlinear phononic crystals. Nanotube based films have been reported to exhibit a supercompressible foamlike behavior under compressive cycling loads.<sup>5</sup>

Carbon nanotubes (CNTs) since their discovery<sup>6</sup> have been tested for many potential applications. Theoretical and molecular-dynamics analyses have been used extensively to study the mechanical response of individual nanotubes under axial and radial deformations.<sup>7–10</sup> Experimental measurement and theoretical studies have agreed in attributing to CNTs an extremely high elastic modulus ( $E$ ), about 1 TPa,<sup>11,12</sup> and mechanical robustness. There have been a number of studies on the nonlinear elastic properties, stability, yielding, and fracture of CNTs (Refs. 8–11 and 13–17) as well as on the low strain rate response of bundles of nanotubes under pressure.<sup>5,18–20</sup>

In this article we present the results obtained by drop-ball testing<sup>3,4</sup> a foamlike forest of aligned coil-shaped carbon nanotubes (CCNTs). This simple method had been proved in the past to enable determining the high strain rate response to impact of a thin layer of nanotubes, allowing measurement and calculation of force-displacement relations for high

strain rate penetration processes at displacements as small as a few microns. The results of this work indicate that coiled carbon nanotubes add a nonlinear spring response to their exceptional elastic stiffness and resilience that makes them suitable for protection of devices from impact.

The elastic contact interaction between a ball and a planar surface, both being linear elastic solids, is regulated by the Hertzian interaction law describing forces at one single contact. In it, the force-displacement relationship has no linear part; therefore Hertz law represents the most famous example of strong nonlinearity.<sup>21</sup> Its behavior stems from the variation of the contact area with the applied forces which has been the foundation for the discovery of a different type of wave propagation.<sup>2</sup> Being able to tailor and control changes in the contact interaction of composites or layered materials is a crucial step for achieving proper tuning of dynamic systems. Nanotube arrays, for example, can be used as constituents of strongly nonlinear phononic materials and provide control of the speed and shape of the propagating signals and mitigation of the traveling pulse's amplitudes.

### II. EXPERIMENTS

The arrays of CCNTs ( $\sim 100 \mu\text{m}$  thick) used in this study were grown as in Ref. 22 on bare quartz substrates (1 mm thick) in a two-stage chemical-vapor deposition (CVD) reactor comprising of liquid and gas injectors. Xylene ( $\text{C}_8\text{H}_{10}$ ) and acetylene ( $\text{C}_2\text{H}_2$ ) served as the carbon source. Indium isopropoxide ( $(i\text{-C}_3\text{H}_7\text{O})_3\text{In}$ ) was dissolved in the xylene-ferrocene ( $\text{C}_{10}\text{H}_{10}\text{Fe}$ ) mixture which was continuously injected into the CVD reaction tube ( $\sim 700^\circ\text{C}$ ) at the rate of 1 ml/h. The atomic concentration of Fe in the xylene-ferrocene mixture was held fixed between 0.75 and 1 at %, and the relative concentration of indium isopropoxide was varied systematically to yield catalyst particles with varying catalyst compositions  $R = \text{In}/(\text{In} + \text{Fe})$ . Acetylene at the flow

<sup>a)</sup>Author to whom correspondence should be addressed; electronic mail: vnesterenko@ucsd.edu

<sup>b)</sup>Present address: Department of Materials Science and Engineering, Carnegie Mellon University, Pittsburgh, PA 15213.

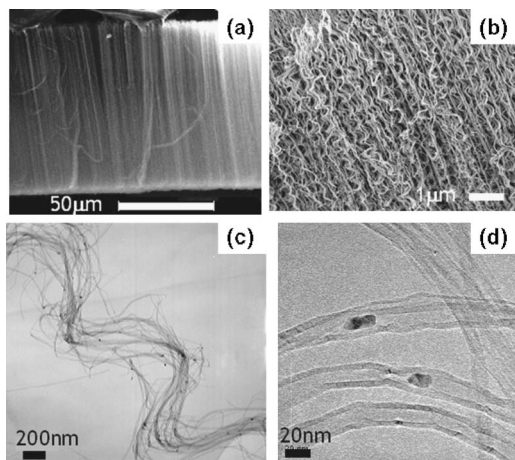


FIG. 1. [(a) and (b)] Low and high magnification SEM pictures showing as-grown forest of coil-shaped carbon nanotubes (CCNTs) used for the experiments. [(c) and (d)] Low and high magnification TEM images of a loose single bundle of the CCNTs.

rate of 50 SCCM (SCCM denote cubic centimeter per minute at STP) and argon at the flow rate of 800 SCCM were fed into the system during the synthesis. After 1 h reaction, the syringe pump and acetylene injection were shut off and the CVD reactor was allowed to cool to room temperature under flowing argon atmosphere. Various parameters, such as the reactor temperature, gas flow rate, and concentrations of iron and indium, were adjusted to optimize the synthesis condition and details can be found in Ref. 22. Scanning electron microscopy (SEM) (Philips operated at 20 kV) and transmission electron microscopy (TEM) (Jeol 3010 operated at 300 kV) were employed to explore the structure and morphology of the as-grown and tested CCNTs used in this study.

The final foam thickness was about 100  $\mu\text{m}$  [Fig. 1(a)]. In the forest, the CCNTs are arranged in bundles, probably due to van der Waals force attraction between them, of  $\sim 25$  nanocoils with a bundle's diameter of  $\sim 500$  nm [see Figs. 1(b) and 1(c)]. The single coiled nanotubes in the forest had a narrow diameter distribution around 20 nm [Fig. 1(d)] with a coiling pitch of  $\sim 500$  nm [Fig. 1(b)]. The total density of the carbon nanotube forest has been estimated at  $\sim 100$  CNTs/ $\mu\text{m}^2$  from simple geometrical considerations. High resolution TEM analysis showed that the investigated coiled nanotubes have parallel graphene walls and did not exhibit a herringbone wall structure.

The experimental setup for measuring the mechanical response of the contact between the impacting ball and the array of nanotubes is presented in Fig. 2(a). The quartz substrate with the grown film of coiled nanotubes was cut in pieces of  $\sim 25$  mm<sup>2</sup> area. These samples were then positioned on top of a calibrated piezoelectric gauge ( $RC \sim 10^3$   $\mu\text{s}$ ) placed on the top surface of a long, vertical steel rod (waveguide) embedded at the bottom into a steel block to avoid possible wave reverberation in the system. The sensor, protected by a brass cover plate, was then connected to a Tektronix oscilloscope to detect force-time curves during dynamic interaction. Calibration was performed taking into account conservation of linear momentum.

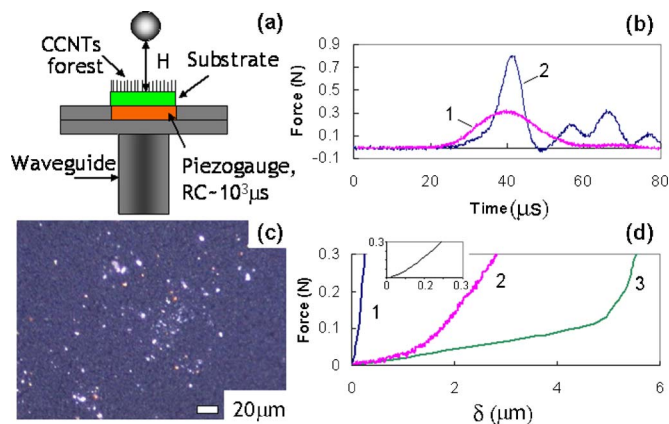


FIG. 2. (a) Schematic diagram of the experimental setup used for testing the forest of carbon nanocoils. (b) Experimentally determined force vs time response obtained for the CCNT forest (curve 1) and the bare quartz substrate (curve 2) when impacted with a 2 mm diameter steel bead (0.02 g) dropped from a height of 2 mm. For a convenient comparison, the time is arbitrarily zeroed to center the curves with respect to each other. (c) Forest of the carbon nanocoils after impact observed under an optical microscope. The area of impact is recognizable by the presence of the white “marker particles” left by the striker during impact. (d) Force-displacement curves derived for the Hertzian contact interaction of the striker ball with the bare quartz substrate [curve 1 based on Eq. (1)], for the contact interaction with the forest of coiled carbon nanotubes (curve 2), and, for comparison, with the forest of microwave plasma grown carbon nanotubes (curve 3) under the same impact conditions (Ref. 4). The inset shows the soft part of curve 1, representing the typical Hertzian behavior at very small displacements.

High strain rate impacts were generated by dropping a stainless steel bead (AISI 316L, 2 mm diameter, mass of  $\sim 0.03$  g) from various heights at room temperature. The calculated velocities of the impacts varied between 0.2 and 2.0 m/s. The strain rate for the lower velocity impacts was estimated in the interval of  $10^4$ – $10^5$  s<sup>-1</sup> from the duration of the impact in the recorded signal ( $\sim 40$   $\mu\text{s}$ ).

The morphology of the nanotube forest surface after impact was analyzed with a Philips SEM operated at 30 kV and with a Nikon Eclipse optical microscope equipped with digital acquisition camera. The impact area was identified using oxide nanoparticles on the impacting bead's surface as a surface stain. During impact the particles remain trapped by the nanocoil forest and function as a marker on the film surface.

### III. RESULTS AND DISCUSSION

The typical contact force-time response after a small amplitude impact (0.2 m/s striker velocity) on the surface of the film is shown in Fig. 2(b), curve 1. Repeated experiments demonstrate identical behavior of contact force. For comparison, the contact response on the bare quartz wafer under identical impact conditions was also measured and presented in Fig. 2(b), curve 2. The presence of the coiled carbon nanotube foamlike array appeared to dramatically change the slope of the contact force and attenuate the amplitude of the pulse. A perfectly elastic response is also noticeable from the symmetry of curve 1: the value of the coefficient of restitution ( $e \sim 1$ ) for the nanocoil film can be calculated from the dependence of the contact force on time during the penetration stage (from the beginning of interaction to the peak of curve 1) and the restitution stage (from the peak to the bot-

tom of curve 1). The image of the forest's surface after impact is shown in Fig. 2(c). It is evident that the forest of nanocoils exhibits a full recovery after the elastic deformation caused by the impact. This is in contrast to our previous results where the forest of straight multiwalled nanotubes was fractured into small fragments with the sizes comparable to the diameter of nanotube<sup>3</sup> or permanently deformed.<sup>4</sup>

The corresponding contact force-displacement curve ( $F$ - $\delta$ ) was constructed based on the initial velocity and the measured dependence of force on time and shown in Fig. 2(d). We compared  $F$ - $\delta$  curves obtained for the Hertzian contact interaction of a steel bead with quartz (curve 1), with the one for the coiled carbon nanotube film (curve 2), and with the response of a film composed of aligned straight CNTs grown in a microwave plasma enhanced CVD system<sup>4</sup> (curve 3). Curve 1 [Fig. 2(d)] was calculated by Eq. (1):

$$F(\delta) = \frac{4E_1E_2\sqrt{R}\delta^{3/2}}{3[E_2(1-\nu_1^2) + E_1(1-\nu_2^2)]}, \quad (1)$$

where  $R$  is the radius of the ball,  $\delta$  indicates the displacement during compression of the film,  $\nu_1$  and  $\nu_2$  are the Poisson coefficients, and  $E_1$  and  $E_2$  are Young's moduli for quartz and steel, respectively ( $\nu_1=0.18$ ,  $\nu_2=0.28$ ,  $E_1=76.5$  GPa, and  $E_2=207$  GPa).<sup>4,23</sup> Curves 2 and 3 were derived from the change of linear momentum due to the impulse of the contact force, allowing the estimation of the ball velocity dependence on time and the calculation of the displacement  $\delta$ . Then of the experimentally detected force  $F$  and the calculated displacement  $\delta$  at the same moment  $t$  were plotted to get  $F(\delta)$  curves as in Ref. 4. Such data on contact interaction might be also used for estimating the elastic properties of the nanocoils.

It is clear from Fig. 2(d) that the coiled carbon nanotube layer exhibits a fundamentally different response of the contact interaction as compared to the bare quartz substrate and the aligned CNT behavior.<sup>4</sup> The total depth of displacement of the striker bead into the nanocoil forest was calculated at  $\sim 3 \mu\text{m}$ , involving an area of interaction with an  $\sim 77 \mu\text{m}$  radius corresponding to an average pressure estimated at  $\sim 16$  MPa. From the SEM and optical microscope analyses [see Fig. 2(c)] no permanent deformation was observed, indicating that the displacement ( $\delta$ ) is the same for the compression and relaxation stages of the coiled carbon nanotube foam. Analogous responses were detected in the full range of striker velocities tested, demonstrating the huge elastic recovery of the nanocoils. To evaluate the nonlinear response of the film impacted by a striker velocity of 0.2 m/s and compare it with the classical Hertzian behavior, we approximated curve 2 with a power law response,  $F=A\delta^m$ , and obtained a qualitative match, for the force range detected in experiments [Fig. 2(b)], at values of  $A=0.031$  and  $m=2.2$  measuring the force ( $F$ ) in newtons and the displacement ( $\delta$ ) in microns. The values of  $m$  for the quartz-steel Hertzian interaction is  $m=1.5$ , therefore demonstrating a significantly different type of nonlinear behavior. It is not clear if this highly nonlinear behavior is also connected to the sideways interaction of the compressed nanocoil bundles. A schematic

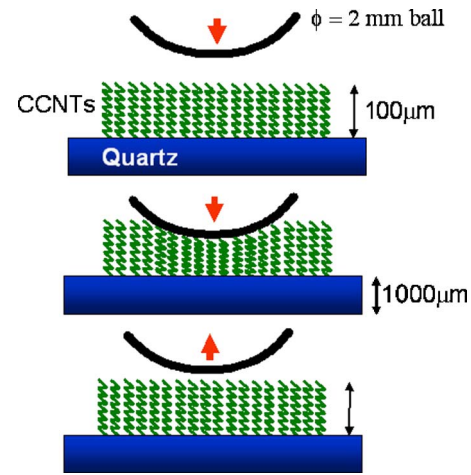


FIG. 3. Schematic diagram showing the stages of interaction and full recovery of the CCNT array during and after the impact.

diagram representing the interaction of the ball with the CCNT film is shown in Fig. 3 for the different stages of interaction.

The results of identical impacts on a different array of multiwall CNTs synthesized by microwave plasma enhanced CVD (Ref. 4) showed a dramatically different behavior [see curve 3 in Fig. 2(d)]. In this case the observed  $F$ - $\delta$  curve presents an abrupt change of the slope at  $\delta \sim 5 \mu\text{m}$  and a much longer depth of striker penetration. Also, for the forest of straight CNTs, SEM analysis showed a permanent plastic deformation and a densification of the impacted area. Analogous testing performed on dc plasma grown CNTs under identical impact condition showed again a different response.<sup>3</sup> In this case the individual tubes showed a uniform fragmentation in segments of 200 nm length, instead of the pure elastic response of the nanocoils or the plastic deformation of the straight microwave grown CNTs.

The differences observed in the dynamic response of the various nanotube foams in comparison with a linear elastic body demonstrate a qualitatively different contact response compared to Hertz law. Such strongly nonlinear CNT films as in the case of the coiled nanotube forest or the other substrates previously tested can be used to create “sonic-vacuum-type” devices<sup>2</sup> serving as nonlinear springs between inertial elements. Applications can be envisioned for designing noise and shock wave mitigation, for impulse transformation, and as mechanical energy storage devices at high strain rate deformation, as suggested earlier for reversible quasistatic compression at similar level of pressures.<sup>19</sup> A similar behavior for a forest of freestanding nanotubes was also reported in Ref. 5 for cyclic compressive loading, showing an excellent recovery and a highly resilient nature of the CNT film even after severe testing conditions.

Another set of experiments was performed on the setup described in Fig. 4(a). In this case, we placed the forest of nanocoils upside down, in direct contact with the sensor's cover plate to monitor the response of the film under uniform planar impact. The striker bead was dropped directly onto the quartz substrate (rigid plate), which transferred the impulsive force to the nanocoils.

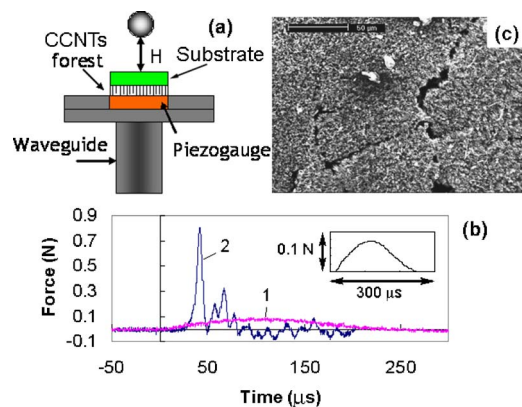


FIG. 4. (a) Schematic diagram of the experimental setup used for testing the forest of carbon nanocoils in an inverted geometry as compared with that described in Fig. 2. (b) Experimentally determined force vs time response obtained for the CCNT forest (curve 1) and the bare quartz substrate (curve 2) when impacted with a 2 mm diameter steel bead (0.02 g) dropped from a height of 2 mm. The inset shows a magnified view of curve 1 for clarity. (c) SEM image showing the fracturing of the surface after repeated high amplitude impacts.

The force ( $F$ )-time ( $t$ ) response of the system to an impact generated by a 2 mm steel bead with an impact velocity of 0.2 m/s is presented in Fig. 4(b) (curve 1) and compared with the pulse recorded impacting the bare quartz substrate (curve 2) as in Fig. 2(b). Interestingly, here the response of the system appears even more efficient in terms of protection of the bottom wall. The amplitude of the pulse detected by the sensor when the nanocoils are present is significantly reduced and the pulse length is increased by almost one order of magnitude. The inset of Fig. 4(b) shows a close-up of curve 1. It is evident that the shape of the curve is not symmetric. This may be due to the effect of tangential forces/sliding of the substrate during impact or presence of dirt particles affecting the behavior of the coiled CNT film.

SEM analysis of the foam surface after several small velocity (0.2 m/s) impacts showed a complete recovery of the film's structure as in the case observed in Fig. 2. After repeated higher velocity impacts (up to 2 m/s) "brittle" cracking of the film substrate began to be noticeable [see Fig. 4(c)]. The cracking was probably related to the detachment of groups of nanocoil bundles from the quartz substrate, forming terraces on the CNT film. Even after cracking, the overall elastic response of the film of carbon nanocoils to the planar impacts did not seem to be heavily effected.

#### IV. SUMMARY

In summary, the mechanical response of a forest of coiled carbon nanotubes under conditions of high strain rate deformation was studied using a simple and convenient experimental approach. It was shown that the deformation of this open foamlike structure of vertically aligned coiled

nanotubes under vertical impacts exhibits a strongly nonlinear, non-Hertzian-type contact interaction law, which could allow the design of strongly nonlinear phononic devices with tunable properties. The nanocoils responded to dynamic loading as perfect elastic nonlinear springs that fully recover their original lengths under all the impact conditions tested. The results also revealed a significant level of amplitude mitigation under high strain rate deformation caused by particles impact. Even after repeated high amplitude impacts, the overall structural elastic response appeared to be conserved, despite the formation of partial cracks on the film's surface. Such a resilient system could find applications in micro-/nanoelectromechanical systems and actuators as well as coating for protection purposes.

#### ACKNOWLEDGMENTS

The authors wish to acknowledge the support for this work provided by the NSF through Grant No. DCMS03013220 (CD, VFN, SJ) and Grant No. DMI-0304019 (AMR).

- <sup>1</sup>L. J. Gibson and M. F. Ashby, *Cellular Solids: Structure and Properties* (Pergamon Press, New York, 1988).
- <sup>2</sup>V. F. Nesterenko, *Dynamics of Heterogeneous Materials* (Springer-Verlag, New York, 2001), Chap. 1.
- <sup>3</sup>C. Daraio, V. F. Nesterenko, J. AuBuchon, and S. Jin, *Nano Lett.* **4**, 1915 (2004).
- <sup>4</sup>C. Daraio, V. F. Nesterenko, and S. Jin, *Appl. Phys. Lett.* **85**, 5724 (2004).
- <sup>5</sup>A. Cao, P. L. Dickrell, W. G. Sawyer, M. N. Ghasemi-Nejhad, and P. M. Ajayan, *Science* **310**, 1307 (2005).
- <sup>6</sup>S. Iijima, *Nature (London)* **354**, 56 (1991).
- <sup>7</sup>S. Iijima, C. Brabec, A. Maiti, and J. Bernholc, *J. Chem. Phys.* **104**, 2089 (1995).
- <sup>8</sup>B. I. Yakobson, C. J. Brabec, and J. Bernholc, *Phys. Rev. Lett.* **76**, 2511 (1996).
- <sup>9</sup>M. R. Falvo, G. J. Clary, R. M. Taylor II, V. Chi, F. P. Brooks, Jr., S. Washburn, and R. Superfine, *Nature (London)* **389**, 582 (1997).
- <sup>10</sup>T. Belytschko, S. P. Xiao, G. C. Schatz, and R. S. Ruoff, *Phys. Rev. B* **65**, 235430 (2002).
- <sup>11</sup>C. Q. Ru, *Phys. Rev. B* **62**, 9973 (2000).
- <sup>12</sup>A. Pantano, D. M. Parks, and M. C. Boyce, *J. Mech. Phys. Solids* **52**, 789 (2004).
- <sup>13</sup>M. Arroyo and T. Belytschko, *Mech. Mater.* **35**, 193 (2003).
- <sup>14</sup>T. Ozaki, Y. Iwasa, and T. Mitani, *Phys. Rev. Lett.* **84**, 1712 (2000).
- <sup>15</sup>C. Wei, K. Cho, and D. Srivastava, *Appl. Phys. Lett.* **82**, 2512 (2003).
- <sup>16</sup>S. P. Chan, W. L. Yim, X. G. Gong, and Z. F. Liu, *Phys. Rev. B* **68**, 075404 (2003).
- <sup>17</sup>B. I. Yakobson, M. P. Campbell, C. J. Brabec, and J. Bernholc, *Comput. Mater. Sci.* **8**, 341 (1997).
- <sup>18</sup>M. J. Peters, L. E. McNeil, J. P. Lu, and D. Kahn, *Phys. Rev. B* **61**, 5939 (2000).
- <sup>19</sup>S. A. Chesnokov, V. A. Nalimova, A. G. Rinzler, R. E. Smalley, and J. E. Fisher, *Phys. Rev. Lett.* **82**, 343 (1999).
- <sup>20</sup>H. J. Qi, K. B. K. Teo, K. K. S. Lau, M. C. Boyce, W. I. Milne, J. Robertson, and K. K. Gleason, *J. Mech. Phys. Solids* **51**, 2213 (2003).
- <sup>21</sup>K. L. Johnson, *Contact Mechanics* (Cambridge University Press, New York, 1985).
- <sup>22</sup>W. Wang and A. M. Rao, *Mater. Res. Soc. Symp. Proc.* **858E**, HH.2.8.1 (2005).
- <sup>23</sup>See [http://www.tydex.ru/materials/materials2/crystal\\_quartz.html](http://www.tydex.ru/materials/materials2/crystal_quartz.html) and [http://www.hoyaoptics.com/specialty\\_glass/fused\\_silica.htm](http://www.hoyaoptics.com/specialty_glass/fused_silica.htm)